Theoretical studies of Rashba and Dresselhaus effects in hybrid organic-inorganic perovskites for optoelectronic applications

Laurent Pedesseau, Mikael Kepenekian, R Robles, Daniel Sapori, Claudine Katan, Jacky Even

▶ **To cite this version:**

HAL Id: hal-01291660

https://univ-rennes.hal.science/hal-01291660

Submitted on 21 Mar 2016

Theoretical studies of Rashba and Dresselhaus effects in hybrid organic-inorganic perovskites for optoelectronic applications

L. Pedesseau*[a], M. Kepenekian[b], R. Robles[c], D. Sapori[a], C. Katan[b], J. Even[a]

[a]Université Européenne de Bretagne, INSA, FOTON UMR 6082, 35708 Rennes, France; [b]Institut des Sciences Chimiques de Rennes, UMR 6226, CNRS – Université de Rennes 1, France; [c]ICN2 - Institut Catala de Nanociencia i Nanotecnologia, Campus UAB, 08193 Bellaterra (Barcelona), Spain

ABSTRACT

In this paper, we propose a description of the Rashba and Dresselhaus effects in hybrid organic-inorganic perovskites (HOP). We recall how the loss of the inversion symmetry together with spin-orbit coupling leads to the loss of the spin degeneracy, effect known as the Rashba and/or Dresselhaus effect depending on the resulting symmetry. This phenomenon is exemplified with formamidinium tin iodide $CH(NH_2)_2SnI_3$ where both Rashba and Dresselhaus effects are present. We show that this effect can be controlled by temperature, as observed for the 2-dimensional HOP Bz_2PbCl_4 (Bz = benzylammonium). On the other hand, an applied external electric field can also tune the amplitude of the spin-splitting as shown on the 3-dimensional HOP $CH_3NH_3PbBr_3$.

Keywords: Rashba, Dresselhaus, hybrid perovskite, spin-orbit coupling, DFT

1. INTRODUCTION

Since 2009, 3-dimensional (3D) hybrid organic-inorganic perovskites (HOP) have emerged as an attractive candidate for solar cell devices due to their high performance, and their easy processability[1–5]. Although 3D materials are very promising, the focus has been on 2-dimensional (2D) HOP for 20 years for applications as field-effect transistor (FET)[6] and light-emitting diode (LED)[7]. Recent calculations based on density functional theory (DFT) have highlighted the presence of a giant spin-orbit coupling (SOC) in lead-based HOP[8–10]. Furthermore, Rashba and/or Dresselhaus spin splittings have been predicted for the HOP systems $CH_3NH_3MX_3$[10–14] (X = I, Br, Cl) and $CH(NH_2)_2SnI_3$[14,15]. Rashba[16] and Dresselhaus[17] effects initially refer to the spin splitting present in zinc-blende and würtzite structures, respectively. Control over spin-dependent band structures is attractive and mandatory to provide potential applications in spintronics[18–21]. In this report, DFT and symmetry analysis have been used to describe these effects in HOP structures. After an overview of the effect of SOC together with the loss of inversion symmetry, we illustrate both Rashba and Dresselhaus effects on the 3D HOP $CH(NH_2)_2SnI_3$. Then, a first example shows temperature-control of the spin splitting in a 2D HOP Bz_2PbCl_4 (Bz = benzylammonium). Finally, control of the spin splitting by an external electric field is shown for the 3D HOP $CH_3NH_3PbBr_3$.

*laurent.pedesseau@insa-rennes.fr

2. RASHBA AND DRESSELHAUS EFFECTS

The SOC is usually treated as a perturbation of the zero-order Hamiltonian H^0. The solutions are the spinors $\phi^0_{n\vec{k}\downarrow}$ and $\phi^0_{n\vec{k}\uparrow}$ with the corresponding eigenvalues $\varepsilon^0_{n\uparrow}(\vec{k})$ and $\varepsilon^0_{n\downarrow}(\vec{k})$. The time reversal symmetry leads to conditions for the eigenvalues: $\varepsilon^0_{n\uparrow}(\vec{k}) = \varepsilon^0_{n\downarrow}(-\vec{k})$ and $\varepsilon^0_{n\downarrow}(\vec{k}) = \varepsilon^0_{n\uparrow}(-\vec{k})$ and the inversion symmetry to additional conditions: $\varepsilon^0_{n\uparrow}(\vec{k}) = \varepsilon^0_{n\uparrow}(-\vec{k})$ and $\varepsilon^0_{n\downarrow}(\vec{k}) = \varepsilon^0_{n\downarrow}(-\vec{k})$. Combining both yields to double spin degeneracy: $\varepsilon^0_{n\uparrow}(\vec{k}) = \varepsilon^0_{n\downarrow}(\vec{k})$. When the inversion symmetry is lost, the spin degeneracy condition is no longer valid except for high symmetry point leading to a band splitting away from this point that characterized Rahsba and Dresselhaus effects[10,22].
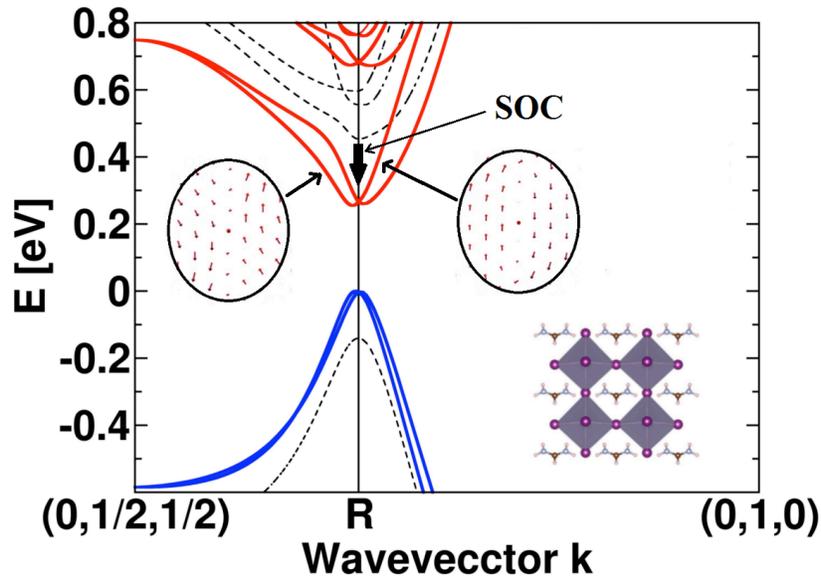

Figure 1. Band structure and spin structures of the conduction band maximum of $CH(NH_2)_2SnI_3$. Blue and red lines are respectively the occupied and unoccupied bands for a calculation including SOC. Black dashed lines are the bands for a calculation without SOC.

Recently, the Rashba effect has been predicted in formamidinium tin iodide $CH(NH_2)_2SnI_3$[15]. The high temperature phase of $CH(NH_2)_2SnI_3$ is the Amm2 phase[15,23]. This space group corresponds to the translation of the ions of the cubic phase along the x and y directions. The resulting point group is C_{2v} with the C_2 axis in the [011] direction. In a quasi-2D system in C_{2v} symmetry, the Rashba-Dresselhaus Hamiltonian[14] reads:

$$H_{RD}(\vec{k}_{//}) = \lambda_R(k_x\sigma_y - k_y\sigma_x) + \lambda_D(k_x\sigma_x - k_y\sigma_y)$$

where λ_R and λ_D refer to the Rashba and Dresselhaus parameters, respectively. Figure 1 represents the band structure computed for $CH(NH_2)_2SnI_3$. The blue and the red lines are the occupied and unoccupied bands for a calculation with SOC to be compared with the black dashed line that are calculated without including SOC. SOC has several consequences. Firstly, it leads to the reduction of the band gap energy. Then, one can observe a splitting of both valence and conduction bands away from the R point. The spin splitting is stronger in the conduction band than in the valence band. As stated above a structure with a C_{2v} symmetry can exhibit both Rashba and Dresselhaus effects. From our calculations, we can extract the following contributions: $\lambda_D^{CBM} = 2.59\ eV/Å$ and $\lambda_R^{CBM} = 0.50\ eV/Å$.

3. TEMPERATURE-CONTROLLED RASHBA EFFECT

In this section temperature control of the Rashba spin splitting is illustrated with the 2D HOP Bz_2PbCl_4 (Bz=benzylammonium)[24]. This 2D HOP (Fig. 2.a) shows a phase transition between 423K and 453 K. From 93 K up to 423 K, the Bz_2PbCl_4 belongs to the $Cmc2_1$ non-centrosymmetric space group, whereas at 453 K it belongs to the Cmca (n°64) centrosymmetric space group[25]. Therefore, the high temperature phase cannot exhibit Rashba nor Dresselhaus effect[14]. On the other hand, the $Cmc2_1$ phase corresponds to a C_{2v} point group for which a spin splitting can be observed. For the non-centrosymmetric phase, the C_2 quantization axis is along the [001] direction. Moreover, the direction [100] corresponds to the stacking direction. Consequently the spin-splitting can be observed only in the [010] direction.

Therefore, the Rashba-Dresselaus Hamiltonian becomes $H_{RD}(\vec{k}_y) = -\lambda_R k_y \sigma_x - \lambda_D k_y \sigma_y$.
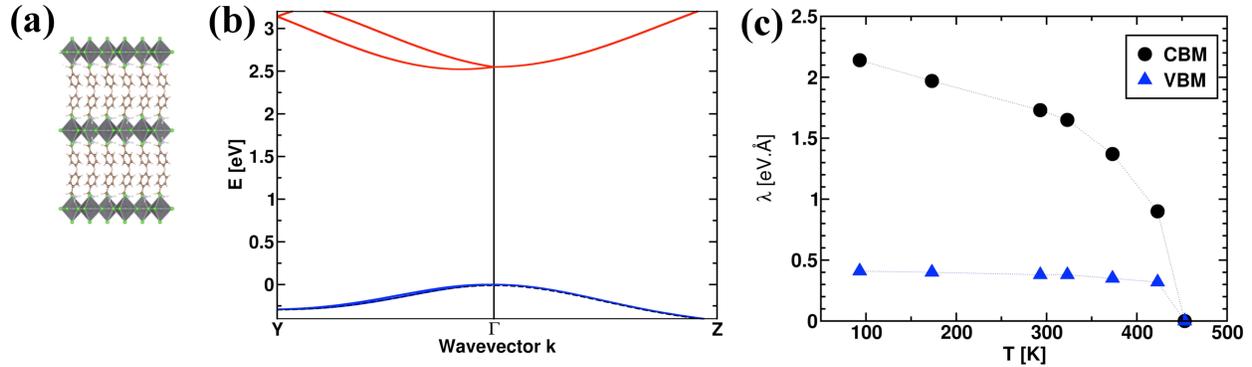

Figure 2. (a) Structure of the 2D HOP Bz_2PbCl_4 (Bz = benzylammonium), (b) band structure of Bz_2PbCl_4 calculated including SOC on the 93 K-structure in the $Cmc2_1$ phase. The blue and the red lines correspond to the occupied and unoccupied bands, respectively. (c) Evolution of the Rashba parameter for the conduction and valence bands with the temperature.

Figure 2.b shows the band structure obtained using the crystal structure recorded at 93 K. A strong spin-splitting is observed in the conduction band (CB) along the Γ→Y direction. No splitting is observed in the Γ→Z direction as it corresponds to the quantization axis. The spin splitting is much stronger in the CB than in the valence band (VB) as illustrated by the Rashba parameters $\lambda^{CBM} = 2.14\ eV/Å$ and $\lambda^{VBM} = 0.41\ eV/Å$. The electronic structure is computed for each structure resolved experimentally at various temperatures. Figure 2.c shows the Rashba parameters for the CB and VB with respect to the temperature. The splitting in the CB strongly depends on the temperature with a decrease from 2.14 eV/Å to 0.90 eV/Å between 93 and 423 K. The variation is quasi linear from 100 to 300 K and then fall drastically until the phase transition to the Cmca space group where no splitting is observed. This variation can be related with the motion of lead atoms along the [010] direction[14]. The VB is also affected, although to a minor extent, by the structural changes with a variation from 0.41 eV/Å to 0.32 eV/Å.

4. RASHBA SPLITTING DRIVEN BY ELECTRIC FIELD

As stated previously, the loss of inversion symmetry is a required condition to obtain a spin-splitting. When the crystal structure presents inversion symmetry, a perturbation such as an external electric field can enforce the loss of this symmetry and reveal the Rashba effect. We analyze here Rashba splitting driven by an applied electric field with the 3D HOP $CH_3NH_3PbBr_3$. This effect has been previously scrutinized on the 3D HOP $CH_3NH_3PbI_3$[14]. The low temperature phase of $CH_3NH_3PbBr_3$ is the Pnma phase[26] which corresponds to a D_{2h} point symmetry (Fig.3.a). Accordingly no spin splitting is observed.
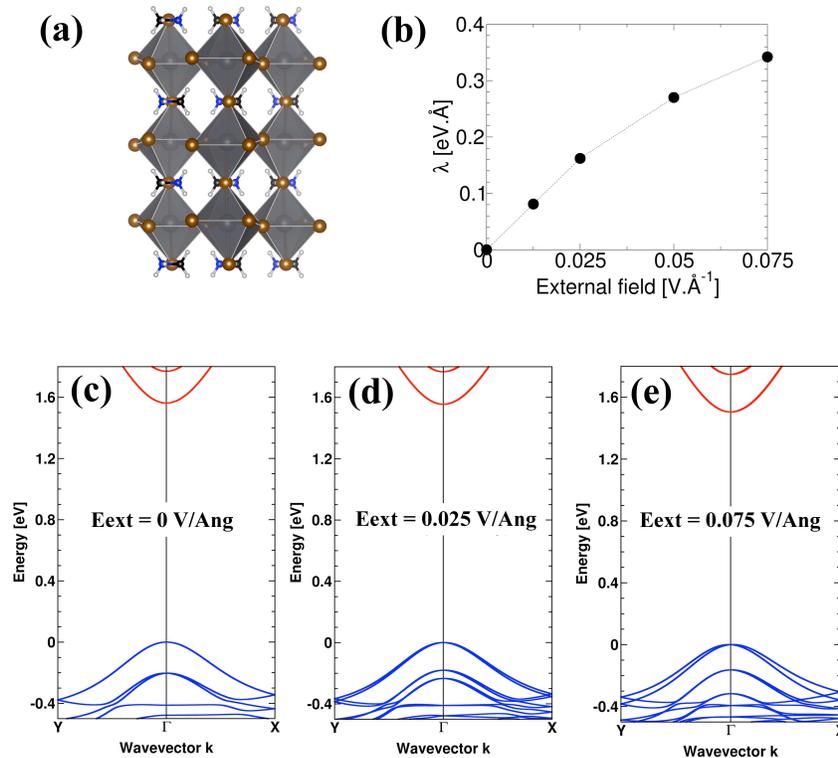
Figure 3. (a) Structure of the 3D HOP $CH_3NH_3PbBr_3$. (b) Evolution of the Rashba parameter of the valence band with the external electric field. (c) Band structure without an external electric field , (c) band structure with an external electric field E_{ext}=0.025 V/Å, and (e) band structure with an external electric field E_{ext}=0.075 V/Å.

We apply a transverse electric field to a slab of $CH_3NH_3PbBr_3$ constructed along the [010] direction and containing three octahedra $PbBr_6$ (Fig. 3.a). Let us notice that when going from the Pnma bulk structure to the slab, the symmetry changes to the centrosymmetric $P2_1/c$ (n°14) space group corresponding to a C_{2h} point group. The band structure for a zero electrical field is shown in Figure 3.c. No spin-splitting is observed because the phase is centrosymmetric. However, when a transverse electric field E_{ext} = 0.025 eV/Å is applied, a spin-splitting appears in the valence band (Fig. 3.d). The splitting is more pronounced for a higher electric field E_{ext}=0.075 eV/Å (Fig 3.e). The evolution of the valence band Rashba parameter in function of the electric field is shown in Figure 3.b. The Rashba parameter increases linearly for low electric field value.

5. CONCLUSION

In summary, Rashba and Dresselhaus effects are described for HOP. We first recall how the combination of time reversal symmetry and inversion symmetry leads to spin degeneracy that is lost when the inversion symmetry breaks. The spin-splitting is illustrated with the formamidinium tin iodide $CH(NH_2)_2SnI_3$ where Rashba and Dresselhaus effects are observed owing to a non-centrosymmetric space group. For structure initially centrosymmetrical, spin-splitting can be induced by an external perturbation. Here we show control of the spin-splitting by the temperature or an external electric field is proposed. A strong variation of the Rashba parameter in the conduction band with the temperature is evidenced for the 2D HOP Bz_2PbCl_4 (Bz = benzylammonium). Finally, the electric-field control of the Rashba effect is treated with the 3D HOP $CH_3NH_3PbBr_3$. The external electric field reveals a possible monitoring of the spin-splitting in the valence band. Such a control of spin precession in HOP materials can lead to spintronics applications.

REFERENCES

[1] Kojima, A., Teshima, K., Shirai, Y., Miyasaka, T., "Organometal Halide Perovskites as Visible-Light Sensitizers for Photovoltaic Cells," J. Am. Chem. Soc. **131**(17), 6050–6051 (2009).

[2] Chen, W., Wu, Y., Yue, Y., Liu, J., Zhang, W., Yang, X., Chen, H., Bi, E., Ashraful, I., et al., "Efficient and stable large-area perovskite solar cells with inorganic charge extraction layers," Science **350**(6263), 944–948 (2015).

[3] Yang, W. S., Noh, J. H., Jeon, N. J., Kim, Y. C., Ryu, S., Seo, J., Seok, S. I., "High-performance photovoltaic perovskite layers fabricated through intramolecular exchange," Science **348**(6240), 1234–1237 (2015).

[4] Matteocci, F., Razza, S., Di Giacomo, F., Casaluci, S., Mincuzzi, G., Brown, T. M., D'Epifanio, A., Licoccia, S., Di Carlo, A., "Solid-state solar modules based on mesoscopic organometal halide perovskite: a route towards the up-scaling process," Phys. Chem. Chem. Phys. **16**(9), 3918 (2014).

[5] Zhou, H., Chen, Q., Li, G., Luo, S., Song, T. -b., Duan, H.-S., Hong, Z., You, J., Liu, Y., et al., "Interface engineering of highly efficient perovskite solar cells," Science **345**(6196), 542–546 (2014).

[6] Kagan, C. R., "Organic-Inorganic Hybrid Materials as Semiconducting Channels in Thin-Film Field-Effect Transistors," Science **286**(5441), 945–947 (1999).

[7] Chondroudis, K., Mitzi, D. B., "Electroluminescence from an Organic−Inorganic Perovskite Incorporating a Quaterthiophene Dye within Lead Halide Perovskite Layers," Chem. Mater. **11**(11), 3028–3030 (1999).

[8] Even, J., Pedesseau, L., Dupertuis, M.-A., Jancu, J.-M., Katan, C., "Electronic model for self-assembled hybrid organic/perovskite semiconductors: Reverse band edge electronic states ordering and spin-orbit coupling," Phys. Rev. B **86**(20) (2012).

[9] Even, J., Pedesseau, L., Jancu, J.-M., Katan, C., "Importance of Spin–Orbit Coupling in Hybrid Organic/Inorganic Perovskites for Photovoltaic Applications," J. Phys. Chem. Lett. **4**(17), 2999–3005 (2013).

[10] Even, J., Pedesseau, L., Jancu, J.-M., Katan, C., "DFT and k · p modelling of the phase transitions of lead and tin halide perovskites for photovoltaic cells," Phys. Status Solidi RRL - Rapid Res. Lett. **8**(1), 31–35 (2014).

[11] Kim, M., Im, J., Freeman, A. J., Ihm, J., Jin, H., "Switchable S = 1/2 and J = 1/2 Rashba bands in ferroelectric halide perovskites," Proc. Natl. Acad. Sci. **111**(19), 6900–6904 (2014).

[12] Brivio, F., Butler, K. T., Walsh, A., van Schilfgaarde, M., "Relativistic quasiparticle self-consistent electronic structure of hybrid halide perovskite photovoltaic absorbers," Phys. Rev. B **89**(15) 155204 (2014).

[13] Amat, A., Mosconi, E., Ronca, E., Quarti, C., Umari, P., Nazeeruddin, M. K., Grätzel, M., De Angelis, F., "Cation-Induced Band-Gap Tuning in Organohalide Perovskites: Interplay of Spin–Orbit Coupling and Octahedra Tilting," Nano Lett. **14**(6), 3608–3616 (2014).

[14] Kepenekian, M., Robles, R., Katan, C., Sapori, D., Pedesseau, L., Even, J., "Rashba and Dresselhaus Effects in Hybrid Organic–Inorganic Perovskites: From Basics to Devices," ACS Nano **9**(12), 11557-11567 (2015).

[15] Stroppa, A., Di Sante, D., Barone, P., Bokdam, M., Kresse, G., Franchini, C., Whangbo, M.-H., Picozzi, S., "Tunable ferroelectric polarization and its interplay with spin–orbit coupling in tin iodide perovskites," Nat. Commun. **5**, 5900 (2014).

[16] Rashba, E. I., "Properties of semiconductors with an extremum loop .1. Cyclotron and combinational resonance in a magnetic field perpendicular to the plane of the loop," Sov Phys - Solid State 2, 1109 (1960).

[17] Dresselhaus, G., "Spin-Orbit Coupling Effects in Zinc Blende Structures," Phys. Rev. **100**(2), 580–586 (1955).

[18] Gregg, J. F., Petej, I., Jouguelet, E., Dennis, C., "Spin electronics a review," J. Phys. Appl. Phys. **35**(18), R121–R155 (2002).

[19] Jansen, R., "The spin-valve transistor: a review and outlook," J. Phys. Appl. Phys. **36**(19), R289–R308 (2003).

[20] Žutić, I., Fabian, J., Das Sarma, S., "Spintronics: Fundamentals and applications," Rev. Mod. Phys. **76**(2), 323–410 (2004).

[21] Jansen, R., "Silicon spintronics," Nat. Mater. **11**(5), 400–408 (2012).

[22] Even, J., "Pedestrian Guide to Symmetry Properties of the Reference Cubic Structure of 3D All-Inorganic and Hybrid Perovskites," J. Phys. Chem. Lett. **6**(12), 2238–2242 (2015).

[23] Stoumpos, C. C., Malliakas, C. D., Kanatzidis, M. G., "Semiconducting Tin and Lead Iodide Perovskites with Organic Cations: Phase Transitions, High Mobilities, and Near-Infrared Photoluminescent Properties," Inorg. Chem. **52**(15), 9019–9038 (2013).

[24] Braun, M., Frey, W., "Crystal structure of bis(benzylammonium) lead tetrachloride, (C7H7NH3)2PbCl4," Z. Für Krist. - New Cryst. Struct. **214**(3) (1999).

[25] Liao, W.-Q., Zhang, Y., Hu, C.-L., Mao, J.-G., Ye, H.-Y., Li, P.-F., Huang, S. D.., Xiong, R.-G., "A lead-halide perovskite molecular ferroelectric semiconductor," Nat. Commun. **6**, 7338 (2015).

[26] Swainson, I. P., Hammond, R. P., Soullière, C., Knop, O., Massa, W., "Phase transitions in the perovskite methylammonium lead bromide, CH3ND3PbBr3," J. Solid State Chem. **176**(1), 97–104 (2003).